Modeling Distributions of Non-Coherent Integration Sidelobes

Joseph J. Rushanan and David W. Winters
The MITRE Corporation

BIOGRAPHY

Dr. Joseph J. Rushanan is a Principal Mathematician in the Signal Processing Section of The MITRE Corporation. He has supported GPS since 1998 and was recently part of the L1C Signal Design Team, where he invented the Weil-based spreading codes. He has published in various areas of discrete mathematics, especially in binary sequences. He received a B.S. and M.S. from The Ohio State University and a Ph.D. from Caltech, all in mathematics. He has been with MITRE since 1986.

Dr. David W. Winters was born in Albany, NY in 1979. He received the B.S. degree from Rensselaer Polytechnic Institute in 2002 and the M.S. and the Ph.D. degrees from the University of Wisconsin-Madison in 2004 and 2007, all in electrical engineering. In 2004, Dr. Winters was awarded a three-year Department of Defense Breast Cancer Research Program predoctoral traineeship. Dr. Winters is currently employed by The MITRE Corporation in Bedford, MA.

ABSTRACT

This paper considers the distribution of the cross-correlation sidelobes from intra-system GNSS interference after non-coherent integration. Because of the inherent periodic structure of the GNSS signals, the successive coherent integrations, while Gaussian distributed, are not independent. We model this dependence in the two separate cases of C/A and L5 signals. We then use the theory of Gaussian quadratic forms to specify the non-coherent integration distribution. Doppler and data bit combinations are shown to have an impact on the form of the distribution. Finally, we consider the special case of a single high-powered interferer. In this case, we use combinatorial reasoning to derive a distribution that is a mixture of all possible distributions for different values of the data bits.

1. INTRODUCTION

The emergence of new and modernized GNSS systems requires useful assessments of the effects of intra- and inter-system interference on a GNSS receiver. Methods that quantify this interference are often based on typical receiver processing operations. Our focus is on the cross-correlation sidelobe distributions at the output of the receiver prompt correlator, which offers a measure that is relevant during signal acquisition. These sidelobe distributions are created separately for each interfering system. The aggregate effect on the correlator output from several such systems can be deduced using assumptions regarding system independence.

Previous work [1] investigated the distribution of cross-correlation sidelobes after coherent integration, since the expected value of the squared-magnitude of these sidelobes is directly related to the spectral separation coefficient (SSC). Focusing on the SSC allows, in almost all cases, the superposition of a set of interfering signals from the same system to be replaced with a single non-repeating white noise random signal [2,3]. This replacement is called the *long-code approximation*.

An exception to the long-code approximation is for C/A on C/A interference, where there are two complementary observations. The first observation is that for longer coherent integrations, e.g., 20 ms, the distribution of the correlator outputs can vary widely depending on location and time. This trait was both modeled and simulated in [1]. That model, which is verified by simulation, explains how the variation in the distribution depends largely on Doppler differences.

The second observation concerns the C/A on C/A sidelobes after integration over a single spreading code period (1 ms). In this case, the long-code approximation holds. However, successive sidelobe values are often correlated. Non-coherently combining these successive values could result in a sidelobe distribution that deviates from the straightforward Chi-square distribution that would be implied by the correlator output values being independent.

Our goal is to quantify the correlation between the successive coherent integrations and determine the distribution from the non-coherent integration. We begin in Section 2 by reviewing the distribution of the single period coherent integrations. We expand the discussion beyond C/A on C/A interference and also consider L5 signals interfering with L5 signals. Section 3 quantifies the correlation between successive correlation outputs. This correlation analysis is first done in the absence of additive thermal noise. However, we also quantify how considering such noise reduces the correlation between the combined correlator outputs.

Section 4 models the distribution of sidelobes for non-coherent integration. The main tool is to consider the overall integration as a Gaussian quadratic form [4-6], where the variables correspond to the individual coherent integrations between the desired signal and one of the interferers. This model yields a distribution that is a weighted sum of independent Chi-square variables.

In Section 5, we apply the model to C/A intra-interference, in particular the non-coherent integration of 20-ms sums. As in the SSC analysis in [1], we see a strong dependence on Doppler difference. We also show how the distribution of 1-ms sums can be approximated as a single Chi-square random variable with a number of degrees of freedom determined by the number of interfering signals. The same techniques show how taking into account additive noise changes the distribution to a different Chi-square distribution.

Finally, in Section 6 we consider the case of a single, high-power interfering signal, i.e., the coherent integrations are dominated by this single signal. In this case, the coherent integrations are restricted to just a few values, and the non-coherent integration will be approximated by a mixture of weighted sum of Chi-square distributions with a reduced number of degrees of freedom.

Section 7 presents our conclusions and recommendations for follow-on work. We include an Appendix A that gives a very brief overview of the GSAT simulator used to verify our models.

2. DISTRIBUTION OF CORRELATION SIDELOBES

Our analysis focuses on receiver processing for acquisition, namely correlation of the desired signal against the received superposition of signals and noise. The fundamental building block for this analysis is the correlation over a single coherent period of the desired signal, or perhaps one component of the desired signal, against a single received signal component or against noise. The resulting correlation value can be modeled as a complex Gaussian random variable.

This modeling technique was used in [1] for the analysis of SSC. In that case, we were interested in the summation of all correlation values, which represents a single coherent integration at the output of the correlator. In this paper, we are concerned with analyzing non-coherent integration, which in turn leads us to the analysis of the dependence of the correlator output as a function of time.

General equations for non-coherent integration are

$$\text{Corr} = \begin{cases} \sum_{n=0}^{N-1} \left|C_n\right|^2 \\ \sum_{n=0}^{N-1} \left|C_n^P\right|^2 + \left|C_n^D\right|^2 \end{cases}, \quad (2.1)$$

where in the top equation, each C_n is the nth coherent integration at the output of the correlator for a single desired signal. In the bottom of Equation (2.1), the separate terms represent contributions from a desired pilot and data components, for example what may used for L5. In both cases, Corr is the total sum of the magnitude squared output of the correlator, which includes all non-coherent and coherent summations over time. We will use the term *sidelobe* for a value of Corr, since we do not consider the case where the desired signal is present in the received signal.

The two separate scenarios of C/A and L5 correlation require some slight differences in the modeling based on Equation (2.1). For each case below, we define the pertinent summands C_n, C_n^P, and C_n^D and the principal random variables that comprise them. In both cases, we use the following assumptions:

- N is the number of non-coherent sums.
- M is the number of interfering signals.
- Unless otherwise stated, the summands do not include additive thermal noise. Additive noise will be considered separately for comparison.
- The spreading codes are periodic, and for a given period, the spreading code values are modeled as random binary variables that are independent for different signals and for different code offsets within the same signal.
- The spreading code values for a single signal are identically distributed Bernoulli trials with mean zero.
- Data bit values for any signal are independent and identically distributed random binary variables.
- Only one sample per spreading code chip is used. For clarity, the techniques, mentioned in [1], that can be

used to extend to multiple samples per chip are omitted from this discussion.
- The Doppler values and integration times are such that we can ignore issues of time dilation in the spreading codes.
- φ_m is the random code phase of the mth interfering signal.
- δ_m is the Doppler difference of the mth signal relative to desired signal. That is, the term reflects subtracting the Doppler value in the desired signal from the Doppler of the mth signal.

Notice that we do not use the actual spreading code values in the model. The reason is that for Doppler differences not close to 0 Hz, the correlation summations using the spreading code and those using random codes will behave the same [1]. In this way, the model focuses on those parameters that have more impact than the spreading code values, such as Doppler and the data bit values. We emphasize that we do use the real spreading codes in the simulations.

2.1 Modeling C/A

For the C/A signal, we have

$$C_n = \sum_{m=1}^{M} \exp(j\varphi_m) \sum_{i=nL}^{nL+L-1} d_{m,i} a_i b_{m,i} \exp(2\pi j \delta_m i / R_1) \quad (2.2)$$

where

- Each C/A signal has spreading period 1023 and chipping rate R_1 = 1023000 chips/s.
- $L = K * 1023$ is the length of the coherent sum, in terms of number of one-sample chips.
- a_i are the (periodic) values of the spreading code for the desired signal. The values are +1/-1.
- $b_{m,i}$ are the (periodic) values of the spreading code for the mth interfering signal. The amplitudes for the mth interferer depend on the received power. However, we will often assume that all the values are all +1/-1 and scale final results. This approach is justified by the narrow range of received power (see [1]). Of course, any simulation results will use the actual received power values.
- $d_{m,i}$ are the values for the data bits of the mth interfering signal. These values are constant +1 or -1 and only change possibly every 20 ms (20460 samples).

The interfering signals also have a delay offset from the desired replica caused by differing radial distances to the satellites. We abstract this offset and assume that the a_i and $b_{m,i}$ start at the same chip. The code offset is then manifested in the $d_{m,i}$ values, since these values are tied to the true start of the interfering spreading. In particular, when the data bit changes, this is likely to occur within a spreading code period.

Due to the periodicities of the signals, the correlator equation is fundamentally composed of 1-ms sums. These sums have only two values (up to sign) for a given m that depend on whether or not there is a bit transition within the 1 ms. If there is no bit transition, which happens at least 19 times out of every 20 ms period, we obtain (up to sign):

$$\sum_{i=k\cdot 1023}^{k\cdot 1023+1022} a_i b_{m,i} \exp(2\pi j \delta_m i / R_1) \,. \quad (2.3)$$

When there is a bit transition, say at some code offset t_m, we obtain (up to sign):

$$\sum_{i=k\cdot 1023}^{k\cdot 1023+t_m-1} a_i b_{m,i} \exp(2\pi j \delta_m i / R_1) - \sum_{i=k\cdot 1023+t_m}^{k\cdot 1023+1022} a_i b_{m,i} \exp(2\pi j \delta_m i / R_1) \quad (2.4)$$

The value of k depends on the index n for the coherent integration and at which 1-ms offset that integration occurs in the case of coherent integration longer than 1 ms. For example, when $K = 1$, we have

$$C_n = \sum_{m=1}^{M} c_{m,n} \exp(j\varphi_m) \exp(2\pi j \delta_m n / 1000) X_{m,n}^{\mathrm{C/A}}. \quad (2.5)$$

The $c_{m,n}$ represent the sign of the 1-ms sums for that interferer and integration.

Equations (2.4) and (2.5) lead to the following definitions:

$$X_{m,k}^{\mathrm{C/A}} = \begin{cases} X_{m,+}^{\mathrm{C/A}} = \sum_{i=0}^{1022} a_i b_{m,i} \exp(2\pi j \delta_m i / R_1), \\ \qquad \text{no bit transition in } k\text{th 1-ms sum} \\ X_{m,-}^{\mathrm{C/A}} = \sum_{i=0}^{t_m-1} a_i b_{m,i} \exp(2\pi j \delta_m i / R_1) \\ \qquad - \sum_{i=t_m}^{1022} a_i b_{m,i} \exp(2\pi j \delta_m i / R_1), \\ \qquad \text{bit transition in } k\text{th 1-ms sum} \end{cases} \quad (2.6)$$

While the value of k does not appear in the summations, it is implicit in choosing which sum is used.

The $X_{m,k}^{\mathrm{C/A}}$ are random variables over the ensemble of spreading codes and data bits. We have $E[X_{m,k}^{\mathrm{C/A}}] = 0$ and $E[|X_{m,k}^{\mathrm{C/A}}|^2] = 1023$, using the assumptions on the spreading codes and assuming unit magnitude of the spreading code values. Each term of a sum like Equation

(2.3) is independent with zero mean but with a difference variance. Even so, we can use a generalization of the central limit theorem to conclude that $X_{m,k}^{\mathrm{C/A}}$ is a complex Gaussian random variable. In fact, unless the Doppler difference is very near 0 Hz, the real and imaginary parts of $X_{m,k}^{\mathrm{C/A}}$ have variance approximately equal to 1023/2, which implies $E\left[X_{m,k}^{\mathrm{C/A}\ 2} \right] \approx 0$ and that $X_{m,k}^{\mathrm{C/A}}$ is nearly circularly-symmetric.

2.2 Modeling L5

The main difference for modeling L5 is that the non-coherent integration could consist of two separate terms, respectively from the pilot channel and the data channel. That is, from Equation (2.1) we have essentially:

$$\left|C_n\right|^2 = \left|C_n^P\right|^2 + \left|C_n^D\right|^2 \tag{2.7}$$

Other scenarios may be of interest, such as acquisition using just the 20-ms long pilot signal; in that case we just ignore the second term. These terms are defined by:

$$C_n^P = \sum_{m=1}^{M} \exp(j\varphi_m) \sum_{i=nL}^{nL+L-1} p_i\, a_i^P \left(d_{m,i}^P b_{m,i}^P + j d_{m,i}^D b_{m,i}^D \right) \exp(2\pi j \delta_m i / R_{10})$$

$$C_n^D = \sum_{m=1}^{M} \exp(j\varphi_m) \sum_{i=nL}^{nL+L-1} a_i^D \left(d_{m,i}^P b_{m,i}^P + j d_{m,i}^D b_{m,i}^D \right) \exp(2\pi j \delta_m i / R_{10}) \tag{2.8}$$

where

- Each L5 signal comprises both a pilot and data component, with spreading period 10230 and chipping rate R_{10} = 10230000 chips/s.
- $L = K * 10230$ is the length of the coherent sum in terms of number of one-sample chips.
- a_i^P and a_i^D are the (periodic) values of the spreading codes for the pilot and data components respectively of the desired signal. Their values are +1/-1.
- $b_{m,i}^P$ and $b_{m,i}^D$ are the (periodic) values of the spreading codes for the pilot and data components respectively of the *m*th interfering signal. Their amplitudes are equal and depend on receive power. As with C/A code, we will often use values of +1/-1 in the analysis.
- $d_{m,i}^P$ and $d_{m,i}^D$ are the values for the pilot and data bits respectively for the *m*th interfering signal. These values are constant +1 or -1 and only change possibly every 10230 samples.
- p_i are the values for the pilot bits of the desired signal, i.e., the length 20 Neuman-Hoffman code. These values are not needed when $K = 1$

As with the C/A model, the bit transitions are abstracted to occur at some point during the spreading code period.

Equation (2.6) defines for C/A two types of variables for each interferer based on 1-ms sums and depending whether a bit transition occurred during the correlation. For L5, the corresponding variables are also 1-ms long, and there are analogously 8 possible variables (up to sign). These variables depend on whether the pilot or data component is desired, whether the pilot or data component of the interfering is considered, and whether or not there is a data (or pilot) bit transition. They are denoted by:

$$X_{m,k}^{P,P}, \quad X_{m,k}^{P,D}, \quad X_{m,k}^{D,P}, \quad \text{and} \quad X_{m,k}^{D,D}, \tag{2.9}$$

where the first superscript indicates the component of the desired signal and the second superscript the component of the interferer. The two possible choices for each variable based on bit transitions are implicitly determined by *k*. As an example,

$$X_{m,k}^{P,D} = \begin{cases} \sum_{i=0}^{10229} jp_i\, a_i^P d_{m,i}^D b_{m,i}^D \exp(2\pi j \delta_m i / R_{10}), \\ \qquad \text{no bit transition in } k\text{th 1-ms sum} \\ \sum_{i=0}^{t_m-1} jp_i\, a_i^P d_{m,i}^D b_{m,i}^D \exp(2\pi j \delta_m i / R_{10}) \\ \qquad - \sum_{i=t_m}^{10229} jp_i\, a_i^P d_{m,i}^D b_{m,i}^D \exp(2\pi j \delta_m i / R_{10}), \\ \qquad \text{bit transition in } k\text{th 1-ms sum} \end{cases} \tag{2.10}$$

Similar conclusions as with the C/A variables hold for these variables, namely they are nearly circularly-symmetric-complex Gaussian variables (provided the Doppler difference is not near 0 Hz) with: $E[X_{m,k}^{\bullet,\bullet}] = 0$, $E[|X_{m,k}^{\bullet,\bullet}|^2] = 10230$, and the real and imaginary parts of $X_{m,k}^{\bullet,\bullet}$ have variance approximately equal to 10230/2, which implies $E\left[X_{m,k}^{\bullet,\bullet\ 2} \right] \approx 0$ (here "$\bullet$" denotes either *P* or *D*).

2.3 Comments on Independence

It is reasonable to assume that the above random variables are independent for different interferers and for different signal components of the same interferer. What is arguably not as reasonable is the independence between two variables that only differ in whether a bit transition took place, i.e., $X_{m,+}^{\mathrm{C/A}}$ and $X_{m,-}^{\mathrm{C/A}}$. The correlation between such a pair of variables is a function of the code delay for the bit transition. Code delays near the center of

a spreading code period will produce variables close to independent, while code delays near 0 will make the variables almost identical (up to sign). Having noted this subtlety, we will regardless continue to assume all of the variables are independent in the analysis. While the full impact of this assumption is still to be assessed, the agreement of the model with simulation would imply that the impact is not appreciable.

3. THE DEPENDENCE OF SUCCESSIVE COHERENT INTEGRATIONS

This section analyzes the correlation coefficient between successive coherent integrations using the 1-ms variables as building blocks. These results were presented briefly in [1] for C/A code, e.g., the correlation between C_n and C_r. That discussion is extended to correlation between $|C_n|^2$ and $|C_r|^2$ and also to L5, i.e., the correlation between $\left|C_n^P\right|^2+\left|C_n^D\right|^2$ and $\left|C_r^P\right|^2+\left|C_r^D\right|^2$. For both cases, we also discuss the whitening effect when the coherent integrations include additive thermal noise.

In general, for real random variables Z_1 and Z_2, we define the correlation coefficient as

$$\rho=\frac{\mathrm{Cov}(Z_1,Z_2)}{\sqrt{\mathrm{Var}\ Z_1\ \ \mathrm{Var}\ Z_2}}. \qquad (3.1)$$

If Z_1 and Z_2 represent two zero mean complex random variables, then the complex correlation coefficient is defined by

$$\rho=\frac{E(Z_1\cdot\bar{Z}_2)}{\sqrt{E(|Z_1|^2)E(|\bar{Z}_2|^2)}}. \qquad (3.2)$$

3.1 C/A Signals

We first consider the case when the coherent integration is 1-ms, that is L = 1023. We focus on C_n as defined by Equation (2.2) in Section 2.1 and are interested in computing the correlation coefficient between C_n and C_r, which we denote by $\rho_{n,r}$. Appealing to Equation (3.2), the denominator is easily seen to be 1023M. For the numerator, we use the fact that the individual interferers are independent to obtain

$$E(C_n\cdot\bar{C}_r)=\sum_{m=1}^{M}\exp(2\pi j\delta_m(n-r)/1000)E(X_{m,n}^{\mathrm{C/A}}\cdot\bar{X}_{m,r}^{\mathrm{C/A}}) \qquad (3.3)$$

There are only two possibilities (up to sign) for, e.g., $X_{m,n}^{\mathrm{C/A}}$, which implies:

$$E(X_{m,n}^{\mathrm{C/A}}\cdot\bar{X}_{m,r}^{\mathrm{C/A}})=1023\,c_{n,r}^{(m)},$$

$$\text{where } c_{n,r}^{(m)}=\begin{cases}0, & X_{m,n}^{\mathrm{C/A}}\neq\pm X_{m,r}^{\mathrm{C/A}}\\ \pm1, & X_{m,n}^{\mathrm{C/A}}=\pm X_{m,r}^{\mathrm{C/A}}\end{cases} \qquad (3.4)$$

Putting the numerator and denominators together, we get

$$\rho_{n,r}=\frac{1}{M}\sum_{m=1}^{M}c_{n,r}^{(m)}\exp(2\pi j\delta_m(n-r)/1000). \qquad (3.5)$$

Consider what happens when n and r are close. Then most of the $c_{n,r}^{(m)}$ are likely equal to 1, since there will not yet be a bit transition for the mth interferer. The correlation coefficient is then the average of the Doppler-defined phasors. If a few of the interferers have Doppler difference that are similar (modulo 1000), then we expect that the correlation coefficient could deviate from zero. As n and r get further apart, the $c_{n,r}^{(m)}$ will start to behave more randomly, which should drive the correlation coefficient to zero.

Next consider the case for K = 20, that is the coherent integration is the length of a data bit period. In this case, we have

$$C_n=\sum_{k=0}^{19}\sum_{m=1}^{M}\exp(j\varphi_m)\exp(2\pi j\delta_m(20n+k)/1000)X_{m,20n+k}^{\mathrm{C/A}}. \qquad (3.6)$$

(note the indexing on the variables reflect that they correspond to specific 1-ms long integrations). The numerator for $\rho_{n,r}$ can be computed as

$$E(C_n\cdot\bar{C}_r)=1023\cdot\sum_{m=1}^{M}\sum_{k=0}^{19}\sum_{\ell=0}^{19}c_{20n+k,20r+\ell}^{(m)}\exp(2\pi j\delta_m(20(n-r)+(k-\ell))/1000). \qquad (3.7)$$

The denominator is similar, except we set $n = r$. In this case, the formula can be simplified in terms of multiplicative factor Dirichlet-like functions discussed in [1]. Since different 20-ms time spans will have, on average, half of the interferers with bit transitions, we expect $\rho_{n,r}$ in the 20-ms case to be closer to zero than for the 1-ms coherent integration case.

Figure 1 illustrates how the correlation coefficient can vary by computing it for various lags over a 30 second experiment using the GSAT simulator (see Appendix A). For visualization purposes, we only computed a real correlation coefficient based on the in-phase portion of the correlator output. The figure clearly shows that the 1-ms sums are correlated, while the 20-ms sums slightly less so.

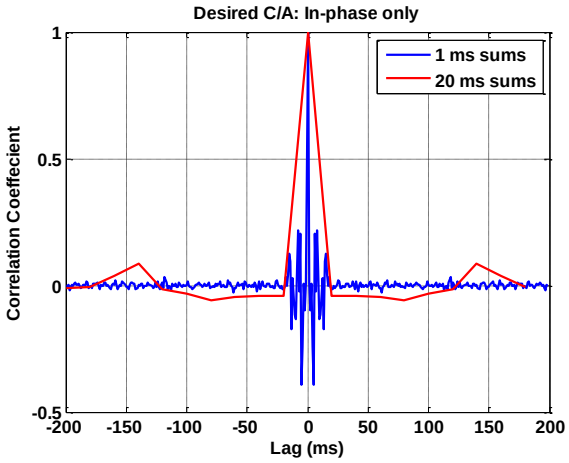

Figure 1. Correlation Coefficient for Various Lags for 1-ms and 20-ms Coherent Sums (C/A Signal; Single 30-sec Simulation)

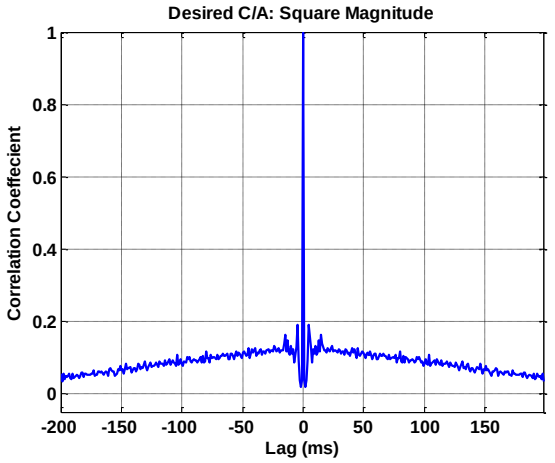

Figure 2. Correlation Coefficient for Various Lags for Squared Magnitude of 1-ms Coherent Sums (C/A Signal; Single 30-sec Simulation)

Next, we compute the correlation coefficient $\rho_{n,r}^{\text{sq}}$ between $|C_n|^2$ and $|C_r|^2$ for the case L= 1023 using Equation (3.1). The properties of circular-symmetry can be used to show that $\text{Var}(|C_n|^2) = (1023\text{M})^2$ and that the covariance between $|C_n|^2$ and $|C_r|^2$ is

$$\left| 1023 \sum_{m=1}^{M} c_{n,r}^{(m)} \exp(2\pi j \delta_m (n-r)/1000) \right|^2 . \qquad (3.8)$$

(recall circular symmetry will hold unless the Doppler difference is near 0 Hz).
Thus

$$\rho_{n,r}^{\text{sq}} = \frac{1}{M^2} \left| \sum_{m=1}^{M} c_{n,r}^{(m)} \exp(2\pi j \delta_m (n-r)/1000) \right|^2 . \qquad (3.9)$$

How does $\rho_{n,r}^{\text{sq}}$ behave? Since each $c_{n,r}^{(m)}$ is likely to be either +1 or -1, because a bit transition only happens at most once every 20 ms, we effectively are looking at the variance of the sum of M random phasors. That value should be M, and so we would expect that $\rho_{n,r}^{\text{sq}}$ should be about $1/M$.

As an example, Figure 2 shows the same experiment as Figure 1, except we calculate the correlation coefficient for the square magnitude 1-ms sums out of the correlator. We see that the correlation stays a fairly flat. In this experiment, M = 8, and the above observation would predict a value of about 1/8, which is consistent with the figure.

3.2 L5 Signals

A similar correlation coefficient analysis can be done for L5 signals, although there are some complications due to the dual components. In this discussion, we focus on only the desired pilot signal. Consider the time series of coherent integrations given just by the $X_{m,k}^{P,P}$ combined with the $X_{m,k}^{P,D}$ variables, then the correlation coefficient takes the same form as Equation (3.5). The main difference is that the corresponding $c_{n,r}^{(m)}$ variables are likely to be 0 more than half the time, up to 7/8ths of the time. The reason is that there are 8 possible combined values of the variables ($X_{m,k}^{P,P} \pm X_{m,k}^{P,D}$); however, the variables are not equally from 1-ms to the next, since only four given values can follow any specific value. This variation in the values is due to the Neuman-Hoffman overlay code and its effect on bit transitions. As such, most of the terms in Equation (3.5) vanish on average, which will dampen the correlation coefficient.

In the case of 20-ms coherent integrations using just the L5 pilot as the desired, note that the 20-ms pilot signal repeats. Thus we have a situation with a periodic length 20*10230 code with no additional overlaid data bits. Correlating the desired pilot against the interfering pilot should have correlation in the 20-ms sums comparable to the 1-ms C/A code. Of course, the additional interfering data component will vary more due to the random data bits, which serves to dampen the correlation in the 20-ms sums. Figure 3 Illustrates these observations for the L5 pilot for the 1 ms and 20 ms case.

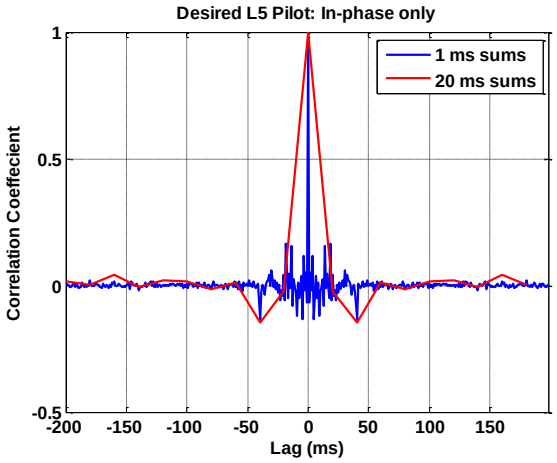

Figure 3. Correlation Coefficient for Various Lags for 1-ms and 20-ms Coherent Sums (L5 Pilot; Single 30-sec Simulation)

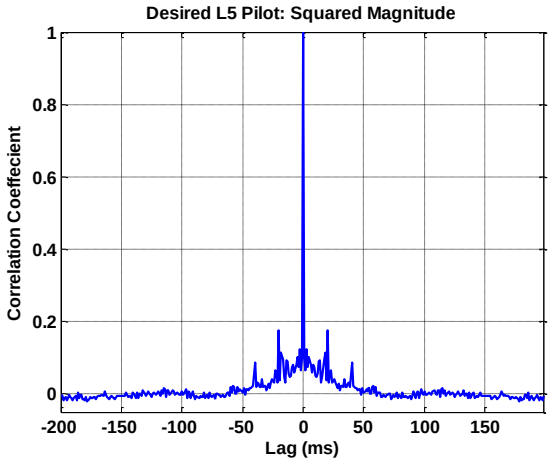

Figure 4. Correlation Coefficient for Various Lags for Squared Magnitude of 1-ms Coherent Sums (L5 Pilot; Single 30-sec Simulation)

Finally, consider the case of squared magnitude for the L5 signals, where again we only consider the contribution of the pilot signal $\left|C_n^P\right|^2$ for $K = 1$. The formula in Equation (3.9) for $\rho_{n,r}^{\text{sq}}$ is relevant, though again what changes is the nature of $c_{n,r}^{(m)}$. Since on average more than half of these values are zero, it is as if we are adding less than half as many random phasors. Thus we expect $\rho_{n,r}^{\text{sq}}$ to be below $1/(2M)$, i.e., half of the value in the C/A case, and perhaps as low as $1/(8M)$. As an example, Figure 4 shows a plot of the squared magnitude correlation coefficient for the same experiment as Figure 2. For this scenario, we have again $M = 8$, which would predict a correlation coefficient around between 1% to 6%.

3.3 The Effect of Noise

In reality, the correlations that we are modeling do not appear in isolation, but as a part of the sum total noise and interference. Since thermal noise can dominate received interfering power, it is reasonable to ask whether thermal noise would serve to whiten the successive correlator outputs.

In general, suppose we have two zero mean random variables Y_1 and Y_2 with correlation coefficient ρ defined as in Equation (3.2). Consider the new variables $Y_1 + Z_1$ and $Y_2 + Z_2$, where Z_1 and Z_2 are zero mean, have respective variances σ_1^2 and σ_2^2, and are mutually independent and independent of Y_1 and Y_2. Then the new correlation coefficient between the new variables is

$$\rho_{\text{new}} = \frac{\rho}{\sqrt{1+\sigma_1^2 \big/ E\ |Y_1|^2 \quad 1+\sigma_2^2 \big/ E\ |Y_2|^2}}. \quad (3.10)$$

In particular, if Y_1 and Y_2 both have variance θ^2 and Z_1 and Z_2 both have variance σ^2, then $\rho_{\text{new}} = \rho/(1+q)$, where $q = \sigma^2/\theta^2$. Thus, for example, if the noise power equals the signal power, we expect the correlation coefficient to be cut in half.

For example, using the same 30 second simulation experiments as in Figure 1, we compare the results with thermal noise of -201.5 dBW/Hz, which gave a value for q of about 3.2. We see that indeed the correlation coefficient is dampened in the presence of noise by about a factor of 4 (= 1 + 3.2).

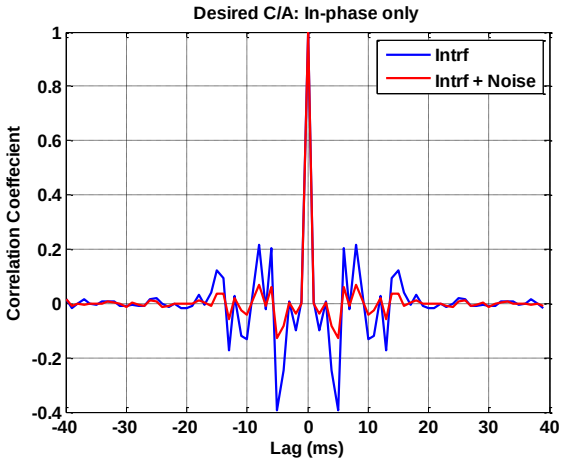

Figure 5. Correlation Coefficient of In-phase 1-ms Sums with Noise Added

4. NON-COHERENT INTEGRATION MODELING: THEORY

In a non-coherent integration such as Equation (2.1), if the summands were the square magnitudes of independent Gaussian variables, we would be able to specify the distribution of the total integration as a Chi-square distribution. However, the correlation coefficient results in the previous section indicate that the distribution of sidelobes from non-coherent integration will likely deviate in some cases from the Chi-square distribution. The goal in this section is to develop tools to quantify this deviation. We will adapt the theory of Gaussian quadratic forms [4-6].

We generalize the derivations in Sections 2 and 3 to give

$$C_n = \sum_{j=0}^{J-1} \alpha_j X_j , \qquad (4.1)$$

where the X_j are independent complex Gaussian random variables and the α_j complex constants. In practice, there are a limited number (up to sign) of X_j, e.g., only two per interferer in the case of C/A code. That means that the total integration depends only on $2M$ independent complex variables, or $4M$ real variables in the case of C/A code. Intuitively we expect that the underlying Chi-square distribution to only have at most $4M$ degrees of freedom, which may be much less than N, the number of non-coherent integrations. Of course, if we also consider summands that include additive thermal noise, then in fact we have possibly $2N + 4M$ variables, since each noise summand produces an independent variable. We discuss the ramifications of noise plus interference at the end of the section.

Let **X** be the row vector of all real variables from the interferers. For C/A code, X has dimension 4M:

$$\mathbf{X} = \left[\mathrm{Re}\ X_{1,+}^{\mathrm{C/A}} , \mathrm{Im}\ X_{1,+}^{\mathrm{C/A}} , \mathrm{Re}\ X_{1,-}^{\mathrm{C/A}} , \mathrm{Im}\ X_{1,-}^{\mathrm{C/A}} , \ldots \right]. \qquad (4.2)$$

Using the appropriate α_j values, e.g., the Doppler and sign terms such as in Equation (2.2), we can write

$$|C_n|^2 = \mathbf{X} A_n \mathbf{X}^\dagger , \qquad (4.3)$$

where the matrix A is an outer product of the real coefficients derived from the α_j and "†" denotes conjugate transpose. Finally, we have

$$\mathrm{Corr} = \sum_{n=0}^{N-1} |C_n|^2 = \mathbf{X} A \mathbf{X}^\dagger , \quad \text{where} \quad A = \sum_{n=0}^{N-1} A_n . \qquad (4.4)$$

A similar analysis works for L5, where **X** has length 16M. Notice, by the way, that we have made no assumption as to the coherent integration length

The matrix A encapsulates all of the Doppler and sign information implicit in Equation (2.2). As such, the distribution implied by Equation (4.4) when all of the variables are considered to be Gaussian variables is essentially a snapshot distribution depending on those Doppler and sign values. As those values change, the distribution changes. In Section 5, we show how the distribution depends on these parameters. We also discuss how one could average these distributions over, say, data bit values. We obtain a probability mixture distribution that would more accurately portray the overall distribution.

Another potential problem with this approach is that we are modeling the 1-ms sums as Gaussian variables even though they can only take on two possible values given the spreading codes and data bit values. To obtain a distribution, we can imagine conceptually re-running the calculation using many different sets of spreading codes and random data. In practice, the mixing of the variables due to the weights in Equation (4.1) serves to make the distribution a reasonable approximation, as confirmed by simulation results.

Once we specify the quadratic form in Equation (4.4), we can apply standard techniques to obtain

$$\mathrm{Corr} = \mathbf{Y} \Lambda \mathbf{Y}^\dagger \qquad (4.5)$$

where **Y** is a vector of independent Gaussian random variables and Λ is a diagonal matrix. This shows that Corr is distributed as a weighted sum of Chi-square random variables each with 1 degree of freedom. When the underlying complex variables are circularly symmetric, which happens approximately when the Doppler difference is not close to 0 Hz, then two of the Y_j variables will have equal weights. That means they can be combined into a single Chi-square variable with 2 degrees of freedom. In general, though, there can be a wide discrepancy between the weights, perhaps by several orders of magnitude.

5. NON-COHERENT INTERGRATION MODELING: EXAMPLES

We apply the techniques in Section 4 to various examples using C/A code. These examples will serve to show the usefulness of the quadratic form technique and the insights it can produce.

5.1 Model versus Simulation

Figure 6 shows how well the model can approach real distributions. By „real distributions" we mean distributions of the correlator outputs using the GSAT simulator. The two plots in the Figure show two different scenarios using the non-coherent integration of ten 20-ms coherent sums, for a total integration time of 200 ms. The two different plots illustrate the variation that can be seen out of the correlator, which is indicative of the variation for 20-ms CA-SSC [1]. In both cases, the model distribution based on the Gaussian quadratic form is a good fit to the experimental distributions. This shows how, the distribution generated by the weighted Chi-square sum can be very close to that achieved experimentally.

5.2 Model Variation

To investigate how the model distributions vary based on parameters, we consider the weights given by the diagonal matrix Λ, which are necessarily non-negative real numbers. For example, for the examples in Figure 6, one possible set of weights is given in Figure 7. For example 1 (the top plot of Figure 6), $M = 9$, so the matrix of the quadratic form is 36 x 36. For the second example, $M = 8$. Notice how many of the weights are essentially inconsequential; indeed these terms are usually ignored when calculating the actual weight sum of Chi-square distribution, as in Figure 6. Also, we see the tendency of the weights to come in pairs. In these experiments, and in what follows, we assume equal amplitude in the interfering signals in order to isolate the other parameter effects.

Figure 7 also demonstrates an interesting relationship between the weights and the shape of the distribution. If the weights are fairly close in size, then the distribution is very narrow, such as example 1 in Figures 6 and 7. The reason is that equal weights would imply a single dominate Chi-square with a low order number of degrees of freedom. On the other hand, if there are only a few very large weights, such as in example 2, then the distribution is very flat. The reason is that we have a single Chi-square with, say, 2 degrees of freedom that is convolved with another weighted sum of Chi-squares with much lower weights. This large size of the first term results in a large range of the overall distribution.

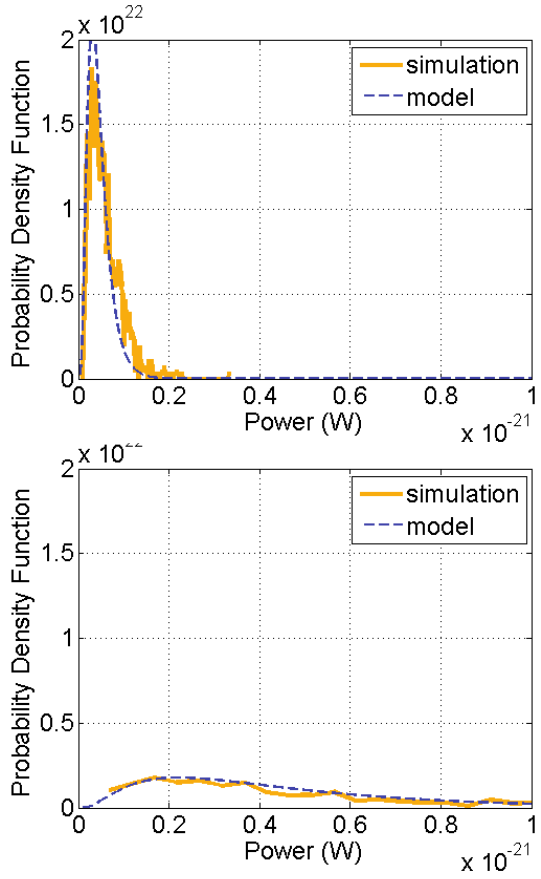

Figure 6. Experimental versus Model Distributions of Correlator Output for 200-ms Non-Coherent Integration of 20-ms Sums Example 1 (top); Example 2 (bottom)

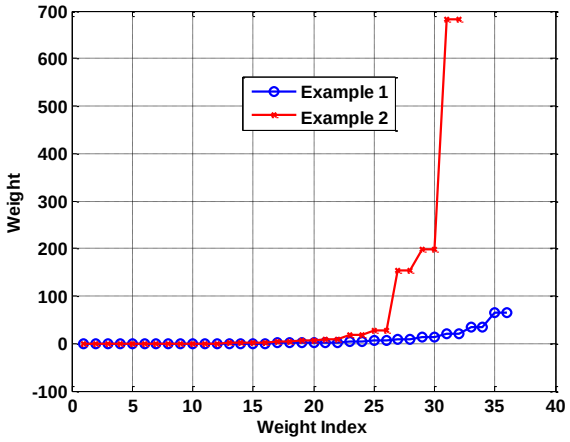

Figure 7. Weights for Diaganolized Quadratic Form for the Examples in Figure 6

The weights used in Figure 7 are one possible set of weights, because while the bit transition and Doppler values were held fixed, we necessarily had to choose bit values randomly. To show the variation that could occur

in the model based on bit values, consider Figure 8. Here we re-ran the model for the two examples used in Figures 6 and 7, except the actual bit values varied. We show 10 different instantiations for each example. While there is variation with the set of ten curves, the overall distributions stay fairly consistent. Thus we can conclude that the modeling technique has some robustness with regard to the bit values.

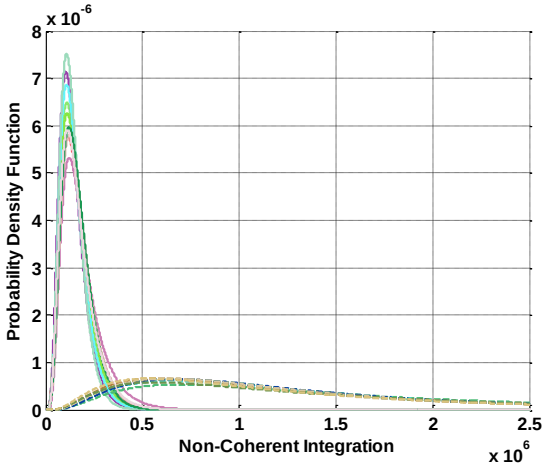

Figure 8. Several Instantiations for Examples in Figure 6
Solid (Example 1); Dashed (Example 2)

Finally, we want to consider the effect of Doppler differences on the case of non-coherently integrating 20-ms coherent sums. Motivated by the analysis in [1], we expect that having many Doppler differences near 0 Hz modulo 1000 Hz should cause the distributions to be much flatter. The reason is that having such numbers implies a large SSC, which in implies a large variance.

Figure 9 supports this observation. Here we ran several experiments where the bit transitions and bit values were held fixed but Doppler was varied. We color code the curves based on how many signals were within +50/-50 modulo 1000 Hz.

The examples in this section used non-coherent integration of 20-ms coherent sums. If we consider non-coherently summing 1-ms sums, we find that in fact the overall distributions look similar for different scenarios. The reason is that even though the successive sums may be correlated, there is not the variation in magnitude that we see due to longer coherent integrations. Of course, the techniques can still be used to yield the non-coherent distributions.

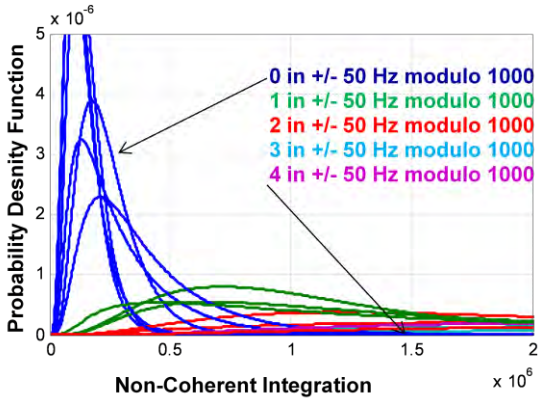

Figure 9. The Effect of Doppler on Non-Coherent Integration Distributions

5.2 Simplifying the Model

The analysis in Section 5.1 offers a simplification for the non-coherent distribution. Because the number of variables in the underlying quadratic forms does not depend on N, we should focus on M to determine a number of degrees of freedom for a given Chi-square. Furthermore, because 19 out of 20 times we use the variable $X_{m,+}^{C/A}$ instead of $X_{m,-}^{C/A}$, we would expect only $2M$ degrees of freedom.

As an illustration, Figure 10 shows the same scenario used in Section 3. The blue curve shows the distribution of non-coherent integration of 1-ms sums for $N = 20$. The approximation to the blue curve is given by

$$\frac{2}{3} \cdot P \cdot \frac{1}{M} \cdot 20 \cdot \frac{1023}{2} \cdot \Delta t^2 \cdot \chi_{2M}, \qquad (5.1)$$

where χ_{df} denotes a real Chi-square random variable with df degrees of freedom. The factor 2/3 compensates for multiple samples per chip in the simulation, Δt is the length of time for a spreading code chip, and P is total interference power, that is we replace all the signal powers with their average. Similarly, the red curve shows the same distribution only additive thermal noise is also considered. In this case, since we have more variables than the dimension of the quadratic form, we expect a full number of degrees equal to $2N = 40$. Indeed, the approximation to the red curve is given as in Equation (5.1) only with $df = 40$.

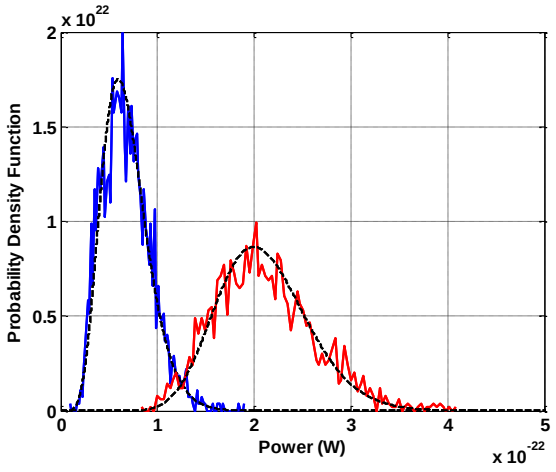

Figure 10. A Simple Chi-Square Approximation to Experiment using 20-ms Non-Coherent Integration of 1-ms Sums
Interference Only (blue); Interference plus Noise (red)

6. NON-COHERENT INTEGRATION WITH SINGLE HIGH POWER INTERFERER

All of the results until now have investigated the impact from several interfering signals. There are times, on the other hand, when considering just a single interferer is useful, e.g., when a single interferer has much higher received power than the other signals. In this case, formulas like Equation (2.5) for C_n reduce to just a single term. While we could apply the quadratic form method to this case, it turns out that it is effective to calculate more directly. The reason is that there is a very limited number of values for C_n, and so the overall distribution is determined combinatorially from the number of each such value.

For example, consider the case of a GNSS signal where the overlay data bit matches the spreading code period. Examples include the L1C pilot and data components and L2C data signal. If we consider just a single such interfering signal, then C_n takes on only two possible values for given Doppler and delay, say X_+ and X_-. The choice of value is random, based on the overlaid data (or pilot) bits. Thus we have

$$\text{Corr} = \sum_{n=0}^{N-1} |C_n|^2 = w|X_+|^2 + (N-w)|X_-|^2. \qquad (6.1)$$

Here w is binomial distributed with success probability 50%, based on the random data bit values. A reasonable probability model for Corr is then a mixture of Chi-square distributions

$$c \cdot \; wY_1 + (N-w)Y_2 \quad , \qquad (6.2)$$

where each Y_1 and Y_2 are independent and identically distributed as χ_2 (using the notation of Equation (5.1)) and c is a scale factor that depends on the variance of the Gaussian variables. The mixture probabilities are derived from the binomial distribution.

This section focuses on the effect of N on this mixture distribution. In practice, one is most interested in the extreme values of the distribution, so the metric used is the tail probabilities as a function of N. We discuss three scenarios: the random noise case, which serves as a benchmark, C/A, L5. To ease the comparisons between the scenarios, we normalize the sidelobe values by the autocorrelation peak of the desired signal.

6.1 Random Noise

In the case of (complex) random noise, each C_n is independent and identically distributed, so that normalized Corr is a scaled version of a Chi-square distribution with $2N$ degrees of freedom:

$$\text{Corr} / \text{Peak} \sim \chi_{2N} / (2LN), \qquad (6.3)$$

where L is the integration length for the coherent integration. This equation follows from the fact that $|C_n|^2$ is distributed as $(L/2)\chi_2$, and the peak is L^2N.

Figure 11 shows how this normalized sidelobe in dB varies in terms of N for L = 10230. Two curves are plotted, one for the 90% cutoff and one for the 99.9% cutoff. Observe that the sidelobe cutoffs decrease with N, albeit slowly.

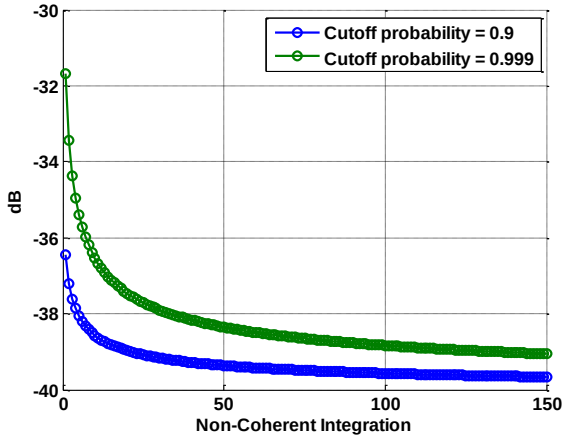

Figure 11. Probability Cutoffs for Non-Coherent Sidelobe Distribution for Random Noise

6.2 C/A Signals

Recall from the discussion of the C/A signal that $|C_n|^2$ will have only two possible values for a single interferer, and that furthermore, one of these values will occur at least 19 out of every 20 times. That means if we let P be floor(N/20), then $N - P$ summands are necessarily identical while the other P summands will be one of the

two types with a 50/50 probability. Thus we get $P + 1$ possible distributions, each of the form

$$wY_1 + (N - P + w)Y_2 \quad / (2LN), \tag{6.4}$$

where $w = 0, \ldots, P$, $L = 1023$, and we use the notation of Equation (6.2).

Figure 12 shows the sidelobe cutoff curves as in Figure 11. Here, though, we see that the cutoffs do not decrease with N. This leveling is to be expected, since Equation (6.4) implies little deviation in the distribution even as N gets large, since one of the two Chi-square terms dominates.

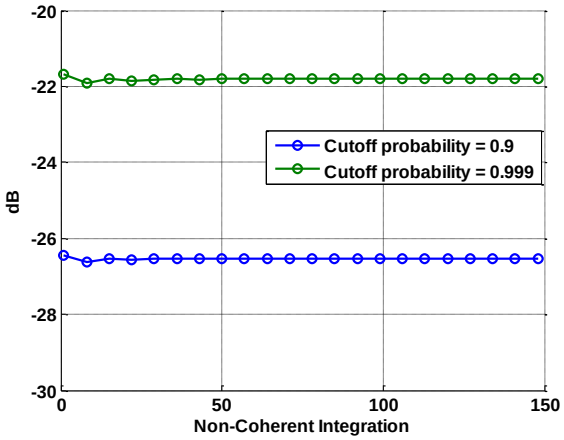

Figure 12. Probability Cutoffs for Non-Coherent Sidelobe for C/A Signal

6.3 L5 Signal

The situation for L5 is more complicated, because there are more possible values for the single summands in the non-coherent sum. Consider $|C_n|^2 = |C_n^P|^2 + |C_n^D|^2$, and look at the possible values for $|C_n^P|^2$. There are eight possible values, based on the bit transitions for the interfering pilot and data component and the actual bit values:

$$\left| X_{\pm}^{P,P} \pm X_{\pm}^{P,D} \right|^2. \tag{6.5}$$

The same holds true for $|C_n^D|^2$, except the choice of bit transitions and bit values is the same as for the pilot terms (because they both are correlating against the same interfering signal). That means the distribution of the normalized Corr is determined by the pattern of these 8 pilot terms and corresponding 8 data terms over the N summands. Observe that for specific bit choices, the distribution of $|C_n|^2$ is a Chi-square distribution with 4 degrees of freedom (since the pilot and data values are independent).

A subtlety that should be considered is that the 8 terms cannot be chosen independently. For example, if the bits one the data component are + and +, then the next pair is either +, + or +, -. In this way, any given term can only be followed by four possible terms. We call this situation the *true bit transition case*. When possible, we will adhere to its restrictions; otherwise, we will treat the terms as independent. Also, we will assume the pilot bits are random, even though they are defined by the length 20 Neuman-Hoffman code.

To mimic the results n Figures 11 and 12 for L5, we need to be able to compute the mixture of the probability distributions based on the patterns of the pilot terms (as we've seen, we only need to focus on the pilot terms). We consider three separate regions based on values of N:

1. For $N \le 10$, we compute combinatorially the exact distribution of all patterns of terms using the true bit transition case and all possible bit values. Each pattern occurs with a given probability determined by its combinatorial strcucture. This probability is used to weight the specific weighted sum of χ_4 in the overall mixture distribution.
2. For $10 < N \le 100$, we compute some number of random patterns of terms. Each pattern occurs with a given probability, which is used to weight the specific weighted sum of χ_4 in the overall mixture distribution. The number of such random patterns is based on achieving a sufficient number of distributions in the mixture calculation. For $N = 16$, we achieve 90% of the weights without difficulty, but for $N = 100$, the threshold is 10%. Even so, the latter case seems to give a reasonable representation of the overall mixture. In this region, we assume the terms are independent.
3. For $N > 100$, we basically assume that all of the possible terms occur the same amount (and thus implicitly are treated as independent). That is, if $N = 8B$, each term occurs B times. In this case, after normalization we approximate the distribution as $\chi_{32}/(16L)$. Notice that this approximation does not depend on N.

We mention that one can also calculate a good approximation to the distributions for region 1 without needing to derive the patterns from all possible bit values. This approximation assumes the terms are independent and uses the set partition formula associated, e.g., with the Faà di Bruno formula [7]. This formula yields an explicit calculation that in turn gives the necessary probabilities of the various types of patterns.

Figure 13 shows the corresponding curves for the L5 case. For each cutoff probability, we plot the results of the three regions. Notice that the flat-line approximation of region

3 appears to be a consistent and reasonable continuation of the other curves.

It is useful to compare Figures 11 and 13. Non-coherent integration is more effective versus random noise due to the fact that successive summands are independent. In the L5 case (as in the C/A case), the limited number of summands implies that the non-coherent sidelobe level off, so that increasing N does not affect the integration.

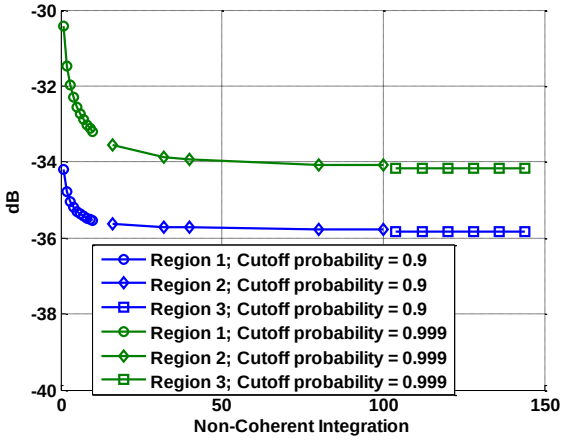

Figure 13. Probability Cutoffs for Non-Coherent Sidelobe for L5 Signal

7. CONCLUSIONS

This paper shows the effectiveness in using simple models of the single signal coherent sums to derive results for non-coherent integration. Some of the insights that can be gained from the model are

- The correlation coefficient of successive 1-ms sums for C/A intra-interference can deviate from zero for small lags. Even when the coherent sums are uncorrelated, the correlation coefficient for the squared magnitudes follows a plateau that depends on the number of interferers.
- The framework of Gaussian quadratic forms can be used to derive distributions of the non-coherent sidelobes. Such analysis leads to simple Chi-square models for situations when a long-code approximation does not hold, for example non-coherently integrating 20-ms sums for C/A intra-interference.
- A combinatorial analysis can be used with the same model building blocks to derive non-coherent sidelobe distributions when only a single interferer is considered. Such results show how the sidelobe values level off for increasing integration length.

While the techniques in this paper were demonstrated for C/A and L5, their application is straightforward to other GNSS signals, such as L1C.

A. APPENDIX: SIMULATION OVERVIEW

We use a numerical simulation that models both a GPS constellation and a simple GNSS receiver at a point on the earth's surface. This simulation is known as GSAT (GNSS Signal Assessment Tool) and was developed by Christopher Hegarty and Michael Tran from the Center for Advanced Aviation System Development (CAASD) at The MITRE Corporation. The GSAT code used in this paper is an updated version of the simulator described in [8].

GSAT consists of an orbital propagator and a simple receiver model. The orbital propagator updates the locations of the satellites in the constellation every 1 ms, which in turn determine the code phase, Doppler, and received power at the receiver location. The receiver model consists of early, late, and prompt correlators (early-late spacing of ½ a chip), which are used by the carrier and code tracking loops to track one of the satellites in view. The prompt correlator output is accumulated and dumped every 1 ms to an output file. The signals are sampled at 4 MHz, although there is no additional front-end filtering. Further details, including specific parameters used, can be found in our previous paper [1].

ACKNOWLEDGMENTS

This work was supported by the US Air Force GPS Wing under contract FA8721-09-C-0001. We gratefully acknowledge the access and assistance of the DoD HPC program.

REFERENCES

[1] Cerruti, A. P., J. J. Rushanan, and D. W. Winters, "Modeling C/A on C/A Interference," Proceedings of ION International Technical Meeting, January 2009.

[2] Betz, J.W., "Effect of Narrowband Interference on GPS Code Tracking Accuracy," Proceedings of ION 2000 National Technical Meeting, Institute of Navigation, January 2000.

[3] Kaplan, E.D., and C.J. Hegarty, eds., *Understanding GPS: Principles and Applications*, 2nd ed., Artech House, 2006.

[4] Tziritas, G.G., "On the Distribution of Positive-Definite Gaussian Quadratic Forms," *IEEE Transactions on Information Theory*, Vol. IT-33, No. 6, November 1987.

[5] Akinniyi, A.R., and J.S. Lehnert, "Characterization of Noncoherent Spread-Spectrum Multiple-Access Communications," IEEE Transactions on Information Theory, Vol. IT-42. No. 1, January 1994.

[6] Biyari, K. H. and W. C. Lindsey, "Statistical Distributions of Hermitian Quadratic Forms in

Complex Gaussian Variables," *IEEE Transactions on Information Theory*, Vol. 39, No. 3, May 1993.

[7] Johnson, W. P., "The Curious History of Faà di Bruno's Formula," American Mathematical Monthly, 109, March 2002, pp. 217-234.

[8] Hegarty, C., and M. Tran, "Compatibility of the New Military GPS Signals with Civil Aviation Receivers, Proceedings AM ION, June 2002.

Modeling Distributions of Non-Coherent Integration Sidelobes

ION ITM 2010
January 26, 2010

Dr. Joe J. Rushanan
Dr. David Winters

The MITRE Corporation

Overview

- **We have developed modeling techniques that quantify dependencies between successive coherent integrations in a GNSS receiver**
  - Specifically for intra-system interference
  - The model uses real parameters (Doppler, etc.)
    - » Using a time-domain approach that handles bit transitions
  - The model provides insights and allows quick “what-ifs”
  - Results applied to C/A and L5 intra-system interference

- **We use the model to**
  - Computing the correlation coefficient between coherent integrations
  - Computing the distribution of sidelobes after non-coherent integration
    - » When all interferers are considered
    - » For the case of a single interferer

Outline

- Model basics
- Correlation coefficient
- Analysis via Gaussian quadratic forms
- The single interferer case
- Conclusions

Background

- **Our model extends previous work for C/A on C/A interference and the behavior of the spectral separation coefficient**

- **There are two main observations from that work**
  - When the coherent integration time is 20 ms
    - » The CA-SSC varies widely by location and time
    - » But successive receiver outputs are uncorrelated
  - When the coherent integration time is 1 ms
    - » CA-SSC follows a long-code approximation
    - » But successive receiver outputs are correlated in time
    - » Thus, distributions of non-coherent integration outputs do not follow the expected distributions

- **This talk addresses the second observation**

Main Correlation Equation

- **Our model is based on this main equation (written for C/A)**
  - *N* = number of non-coherent summands (indexed by *n*)
  - *L* = coherent integration time = *K* x 1023 (one sample per chip)
  - *M* = number of interfering signals (index by *m*)
  - *R* = 1.023 Mchips/s

Replica signal chip values

$$\text{Corr} = \sum_{n=0}^{N-1} |C_n|^2 = \sum_{n=0}^{N-1} \left| \sum_{m=1}^{M} \exp(j\phi_m) \sum_{i=nL}^{nL+L-1} d_{m,i} a_i b_{m,i} \exp(2\pi j \delta_m i / R) \right|^2$$

***m*th interferer phase, data values, chip values, and Doppler difference**
Random code offset is implicit

- **A similar equation is used for L5**
  - Modified to account for both the desired and interfering signals havinhg independent pilot and data components

Model Equation in Pictures

- **The model is constructed via 1-ms correlator sums**
  - Combined coherently and non-coherently

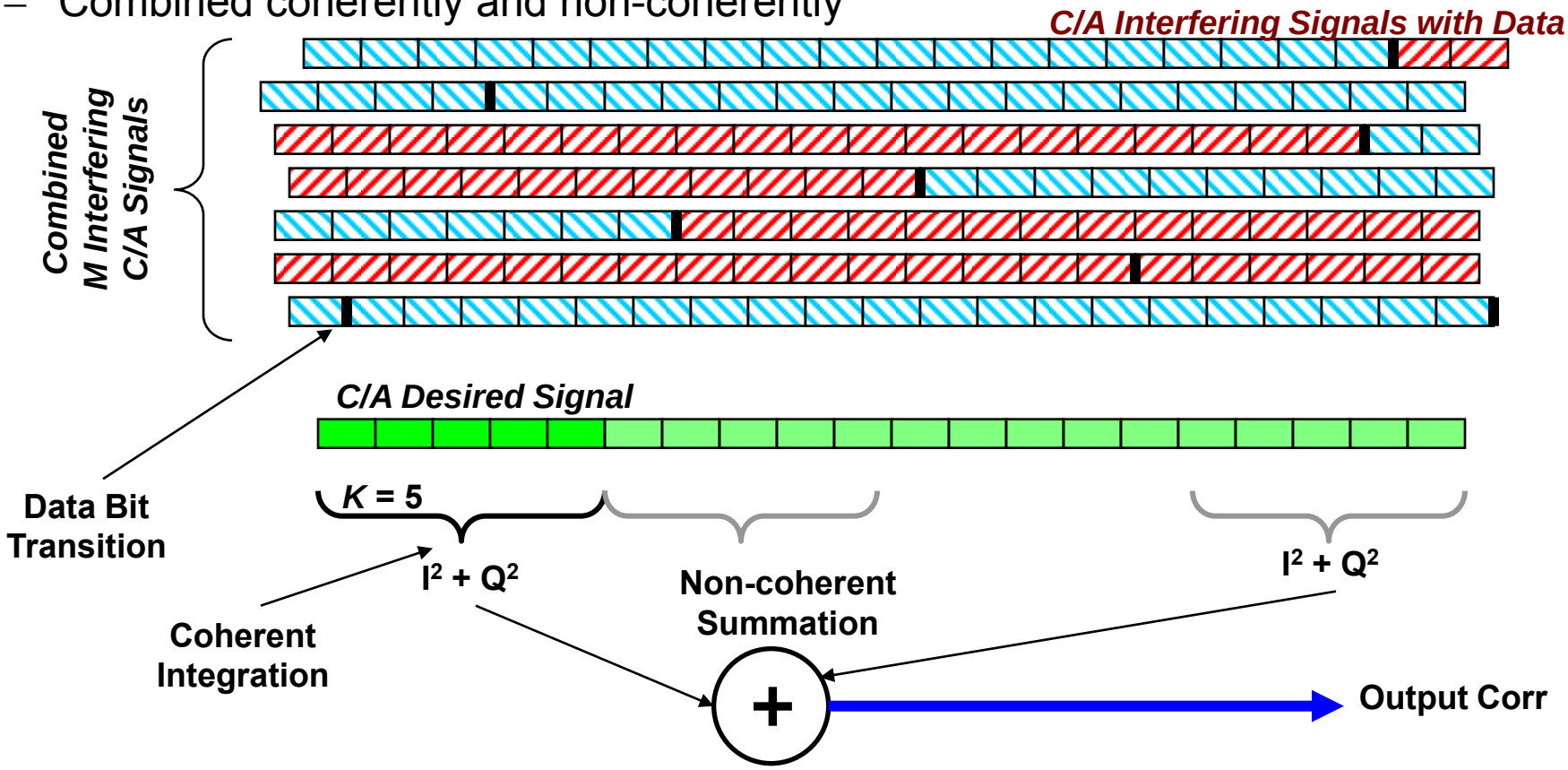

$$\text{Corr} = \sum_{n=0}^{N-1} \left| \sum_{m=1}^{M} \exp(j\phi_m) \sum_{i=nL}^{nL+L-1} d_{m,i} a_i b_{m,i} \exp(2\pi j \delta_m i / R) \right|^2$$

MITRE

The Building Blocks: 1-ms Correlator Sums

- **Break up the 1-ms sums by interferer**
- **Assuming random chips**
  - The real and imaginary parts are Gaussian

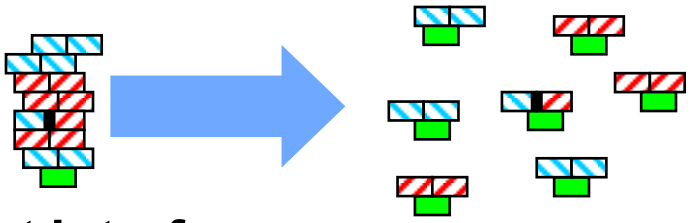

- **These variables are independent for different interferers**
- **For a single interferer, there are two distinct real/imaginary pairs**
  - Based on bit transitions
  - Circularly symmetric for Doppler ≠ 0 Hz
  - Independence depends on where the bit transition occurs

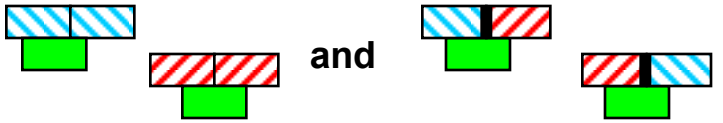

- **For L5, there are 8 variables for each desired pilot and data**
  - Based on the bit transitions on the interfering pilot and data
    - » Due to overlay Neuman-Hoffman codes and data bits
    - » Not equally likely, nor independent in time

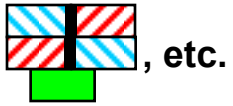

The values for these variables stay the same through the whole integration (up to sign)

Revisiting the Correlation Equation

- **Using the 1-ms sums we can re-write the correlation equation**
- **Here it is for 1-ms coherent integration for C/A**

$$C_n = \sum_{m=1}^{M} s_n^{(m)} \exp(j\varphi_m) \exp(2\pi j \delta_m n / 1000) X_{m,n}^{\mathrm{C/A}}$$

sign

1-ms sums

- **For longer coherent integration, we see the impact of Doppler differences near 0 modulo 1000 Hz**
- **The s_n are constant for 19 out of 20 ms**
  - Which shows why successive coherent integrations are correlated
- **For L5, the similar equations have sign terms that vary each integration**
  - Because of NH codes and data bits

Outline

- Model basics
- **Correlation coefficient**
- Analysis via Gaussian quadratic forms
- The single interferer case
- Conclusions

Correlation Coefficient

- **For the complex correlation coefficient between C_n and C_r**

$$E(C_n \cdot \bar{C}_r) = \sum_{m=1}^{M} \exp(2\pi j \delta_m (n-r)/1000) E(X_{m,n}^{\mathrm{C/A}} \cdot \bar{X}_{m,r}^{\mathrm{C/A}})$$

- **The variables are either equal (up to sign) or independent, yielding**

$$\rho_{n,r} = \frac{1}{M} \sum_{m=1}^{M} c_{n,r}^{(m)} \exp(2\pi j \delta_m (n-r)/1000)$$

- **The $c_{n,r}$ are**
  - 0 if the 1-ms sums are independent
  - +1/-1 if the 1-ms sums are equal or opposite in sign
- **For C/A code, the weights are only zero possibly 1 out of 20 times**
- **For L5, we expect similarly the weights to be zero more than half the time**
  - Up to 7/8ths of the time, if the variables were independent

Correlation Coefficient Example

- **Thus we expect that the correlation coefficient can be large, depending on Doppler values**
- **Plots show correlation coefficient measured using GSAT**
  - Only measuring correlation between in-phase (real) terms

C/A

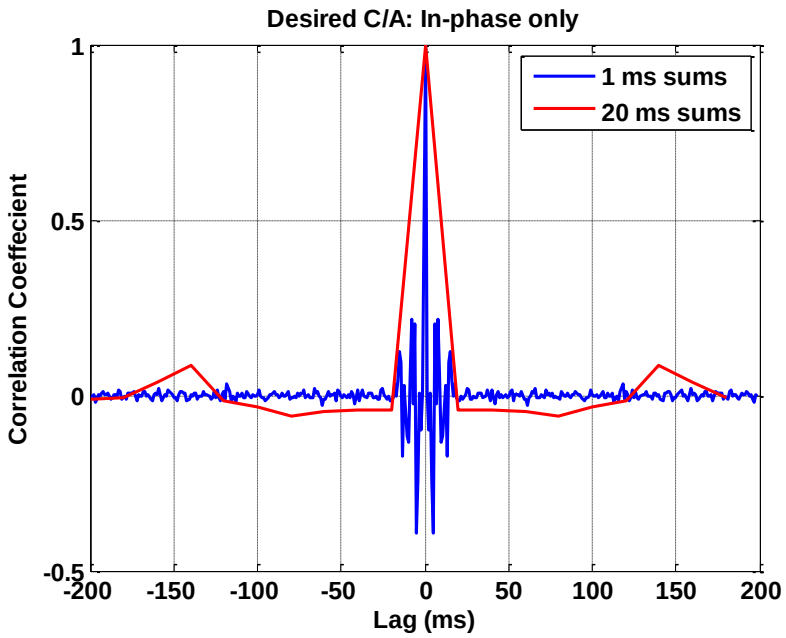

L5

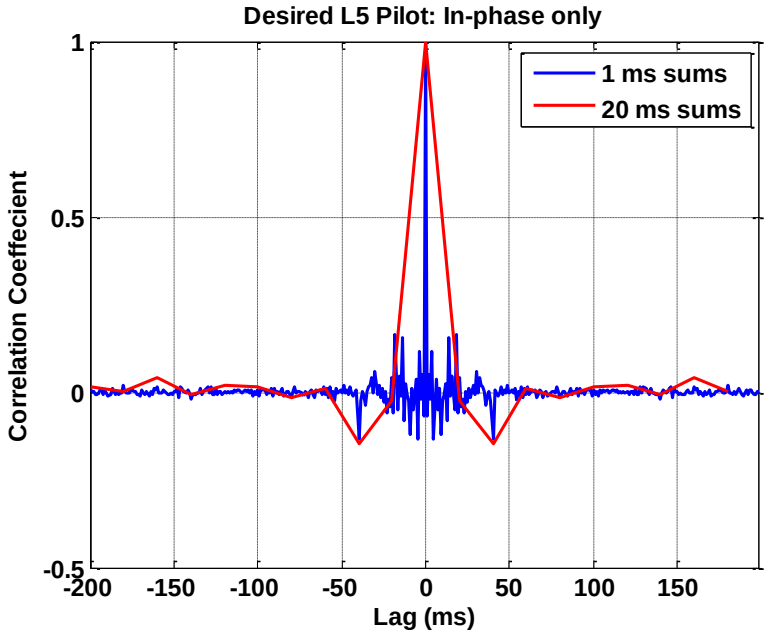

* GSAT was originally developed by Chris Hegarty and Michael Tran of The MITRE Corp.

Correlation Coefficient $I^2 + Q^2$

- **The same techniques can be applied to the correlation coefficient between successive square magnitudes out of the correlator**
  - E.g., correlation of $|C_n|^2$

$$\rho_{n,r}^{\mathrm{sq}} = \frac{1}{M^2}\left|\sum_{m=1}^{M} c_{n,r}^{(m)} \exp(2\pi j \delta_m (n-r)/1000)\right|^2$$

- **For C/A code, we are essentially computing the average variance of a sum of M "random" phasors**
  - So the correlation coefficient behaves like 1/M
- **For L5, since the weights are zero more than half the time**
  - Expect the correlation coefficient to be between 1/(2M) and 1/(8M)

Correlation Coefficient $I^2 + Q^2$ Example

- **Same experiments, looking just at 1-ms sums**
  - M = 8 interferers, so heuristic is about 0.125 and 0.015 to 0.06, respectively

C/A

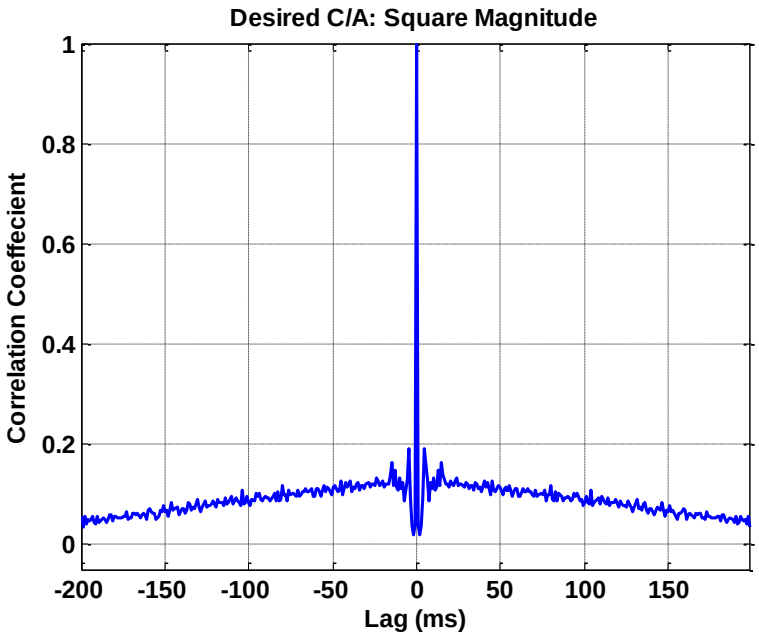

L5

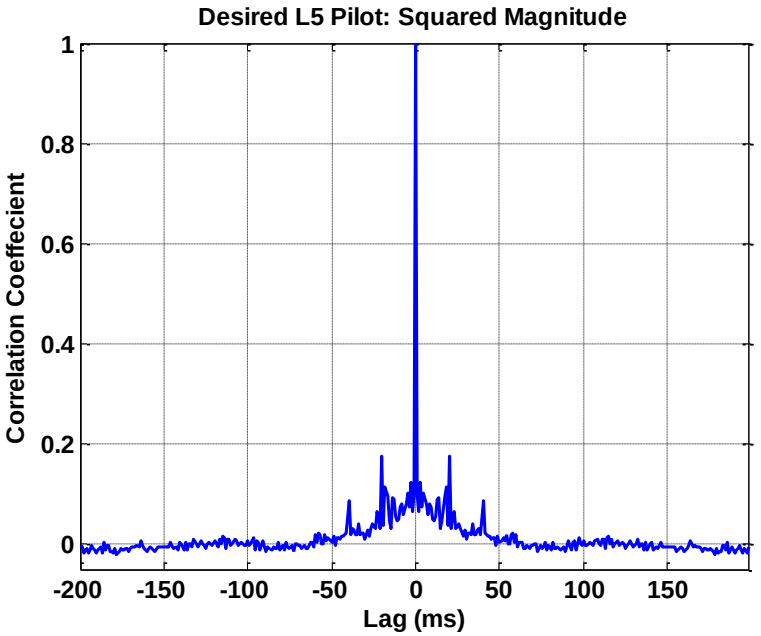

Additive Thermal Noise

- **Consider two cases**
  - Correlation coefficient of just C/A desired versus C/A interference
  - Correlation coefficient of C/A desired versus noise plus C/A interference
- **Let *Q* be the ratio: noise power / (C/A interference power)**
- **Then the correlation coefficient changes as**

$$\rho_{\mathrm{ALL}} = \rho_{\mathrm{C/A}} \left(\frac{1}{1+Q} \right)$$

- **Thus, if Q is unity, the correlation coefficient is halved**

Correlation Coefficient Example
Additive Noise

- **Same experiment, except noise added (-201.5 dB)**
  - Q ~ 3.2, so new coefficient about one fourth of old coefficient

In-phase

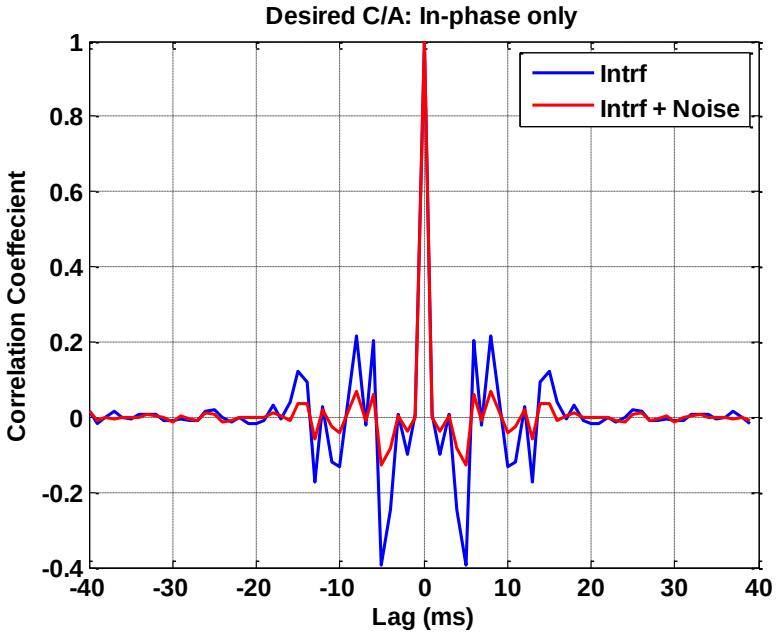

$I^2 + Q^2$

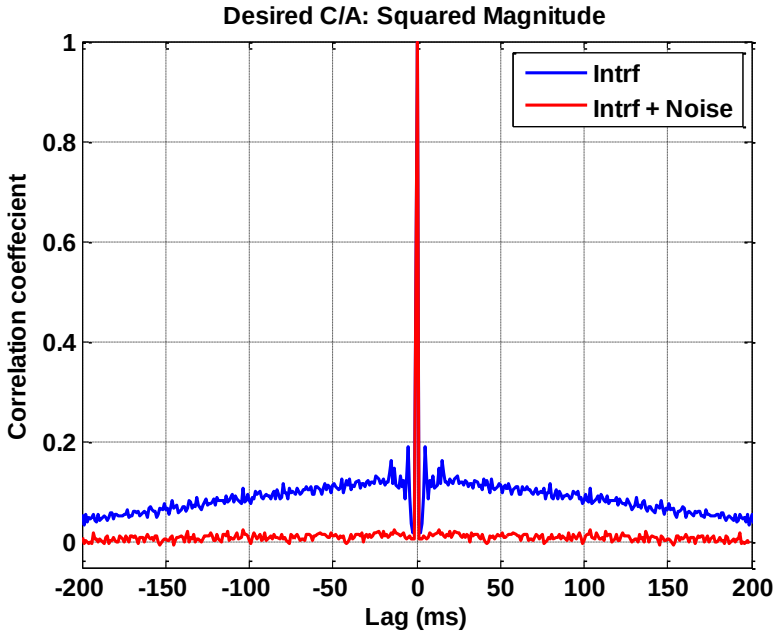

Observations

- **The periodicity of the GNSS signals results in some correlation in successive correlator outputs**
  - Even when all interferers are considered
- **The correlation is diminished when noise is considered**
- **This correlation impacts the non-coherent sidelobe distributions**
- **It also effects any averaging of the correlator outputs, e.g., for example to experimentally measure SSC**

Outline

- Model basics
- Correlation coefficient
- **Analysis via Gaussian quadratic forms**
- The single interferer case
- Conclusions

The Gaussian Quadratic Form

- **A non-coherent integration can be expressed as a quadratic form in the 1-ms (real) Gaussian variables**

$$\text{Corr} = \sum_{n=0}^{N-1} \left| C_n \right|^2 = \mathbf{X} A \mathbf{X}^*, \quad \text{where } A = \sum_{n=0}^{N-1} A_n \text{ and } \left| C_n \right|^2 = \mathbf{X} A_n \mathbf{X}^*$$

- **A_n is a matrix that captures Doppler and sign information**
- **X is a vector of the real variables (+/- = (no bit)/(bit) transition)**

$$\mathbf{X} = \left[\text{Re}\left(X_{1,+}^{\text{C/A}} \right), \text{Im}\left(X_{1,+}^{\text{C/A}} \right), \text{Re}\left(X_{1,-}^{\text{C/A}} \right), \text{Im}\left(X_{1,-}^{\text{C/A}} \right), \ldots \right]$$

- **Diagonalize the form to yield**
  - Each Y_k is an independent Chi-square variable with 1 degree of freedom

$$\text{Corr} \sim \sum_k w_k Y_k$$

The form automatically handles correlation of the 1-ms sums

Example

- **Two experiments for C/A, L = 20 ms, N = 10 non-coherent sums**
  - Created the quadratic form using the Doppler values and bit transitions from the experiment, but with just a single instance of random bit values

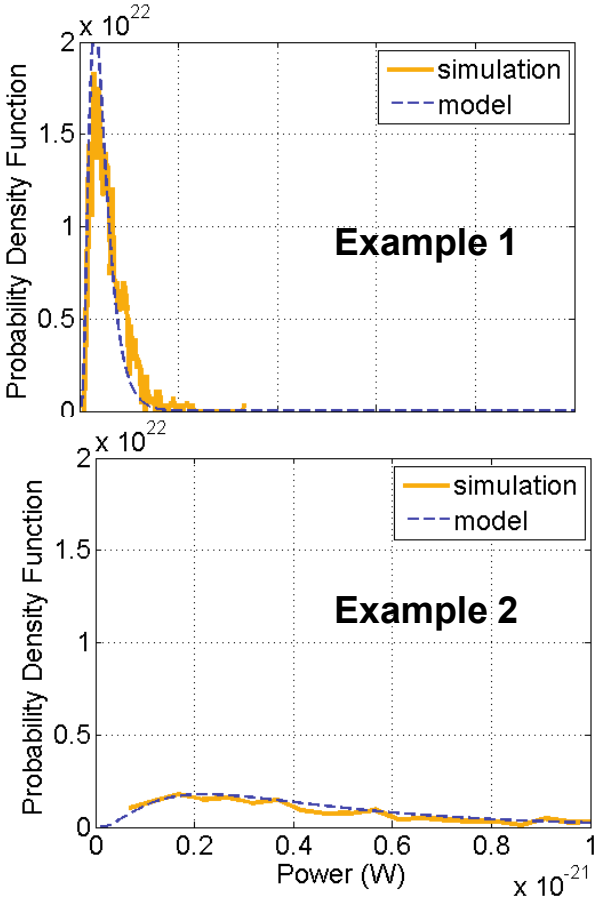

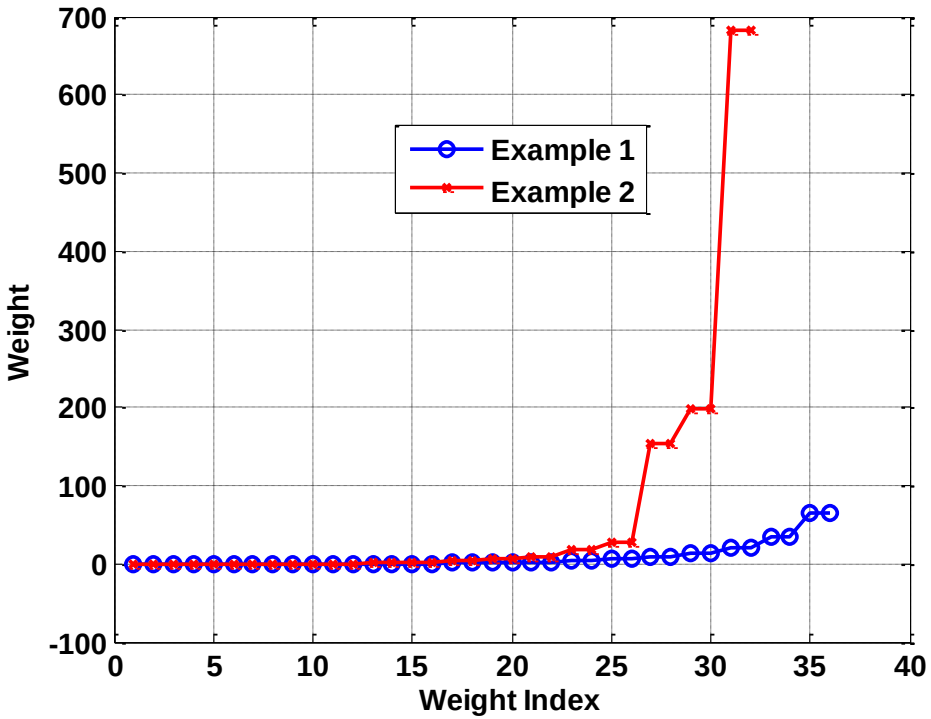

Model Variation

- **The quadratic form depends on the specific parameters**
  - Bit transition locations, bit values, Doppler
- **Changing the bit values varies the distribution somewhat but keeps the same shape**
  - So the true distribution is a mixture distribution over all possible bit values

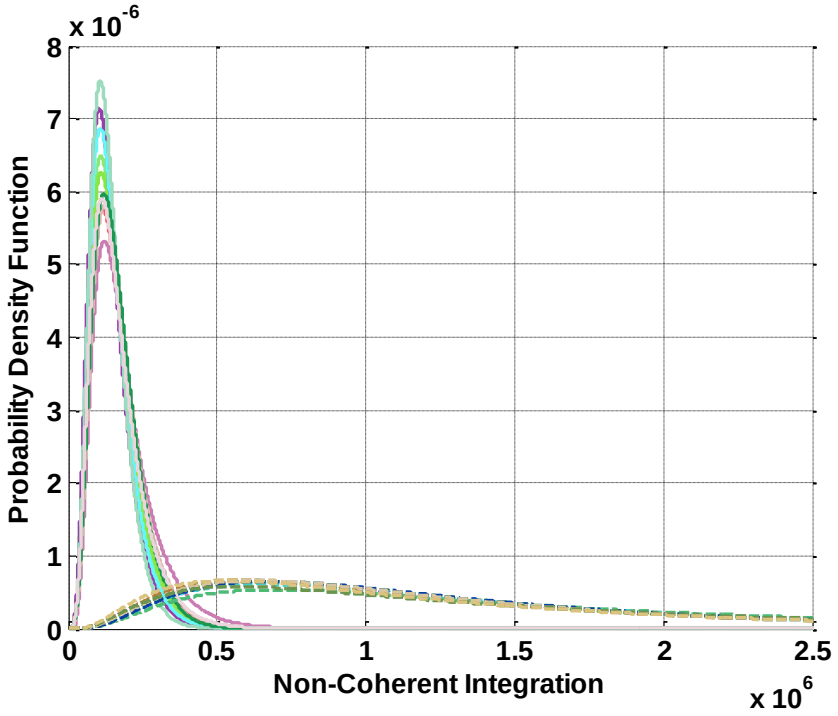

Model and Doppler

- **The form can vary widely based on Doppler values**
  - This is the same effect that gives the variation in CA-SSC
- **For example, these are distributions obtained based on number of Doppler values near 0 Hz modulo 1000 Hz**

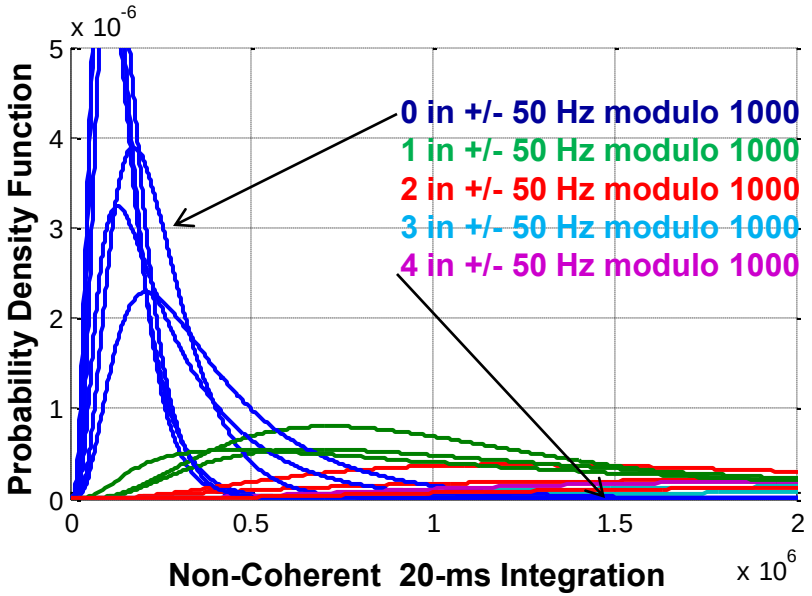

Even Simpler Models

- **Consider C/A, 20-ms non-coherent integration of 1-ms sums**
- **Random interference implies Chi-square with 40 degrees of freedom**
- **But in practice, we only see 2 *M* degrees of freedom**
  - Left is interference only; degrees of freedom = 2 x 8 = 16
  - Right is interference plus noise with 40 degrees of freedom

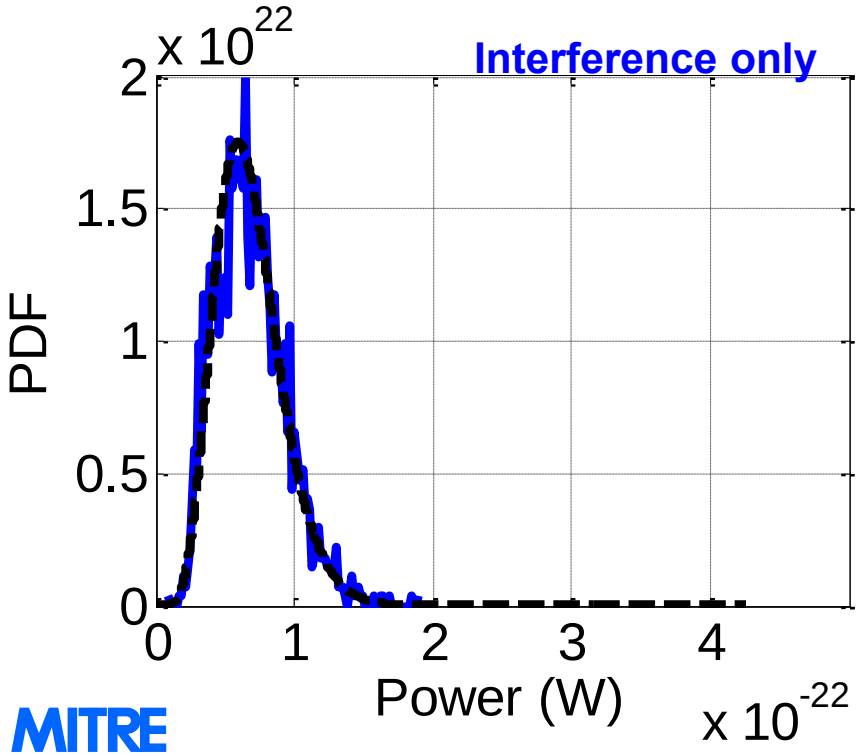

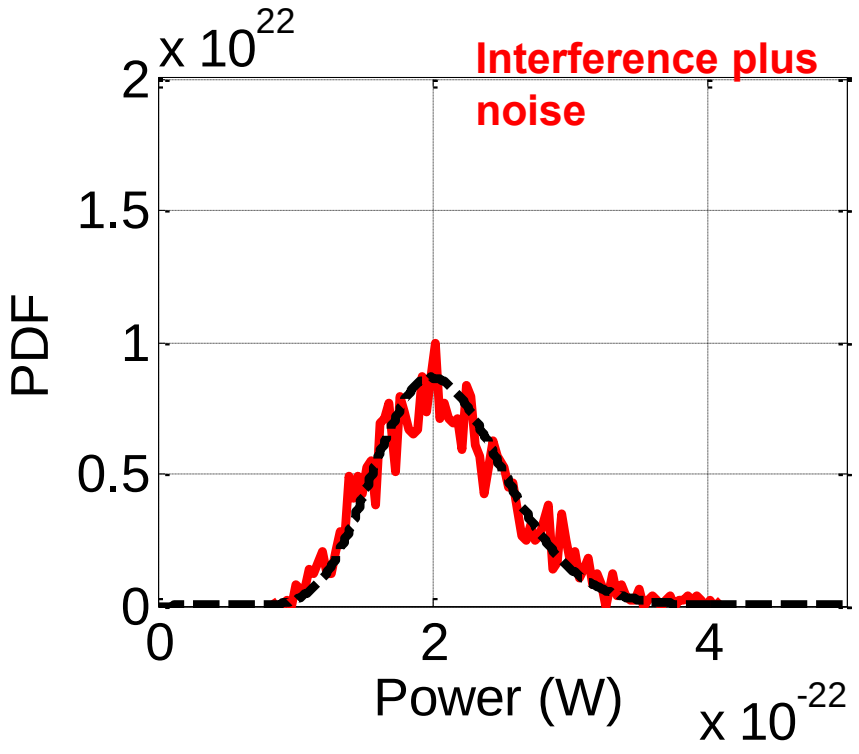

MITRE

Outline

- Model basics
- Correlation coefficient
- Analysis via Gaussian quadratic forms
- **The single interferer case**
- Conclusions

Single Interferer

- **We next consider the distribution of sidelobes for non-coherent integration with only a single interferer**
- **The quadratic form would only have a few variables**
  - Only four for C/A code; sixteen for L5
- **The actual form depends on the combinatorics of the bit transitions**
  - We can reason directly from first principles
- **We look at three cases**
  - A random long-code, C/A, and L5

Long-Code Sidelobe Distribution

- **The distribution of the sidelobes normalized to the autocorrelation peak is $Y / (2 L N)$**
  - Y is Chi-square with $2N$ degrees of freedom
- **The tail cutoffs decrease with N, albeit slowly**

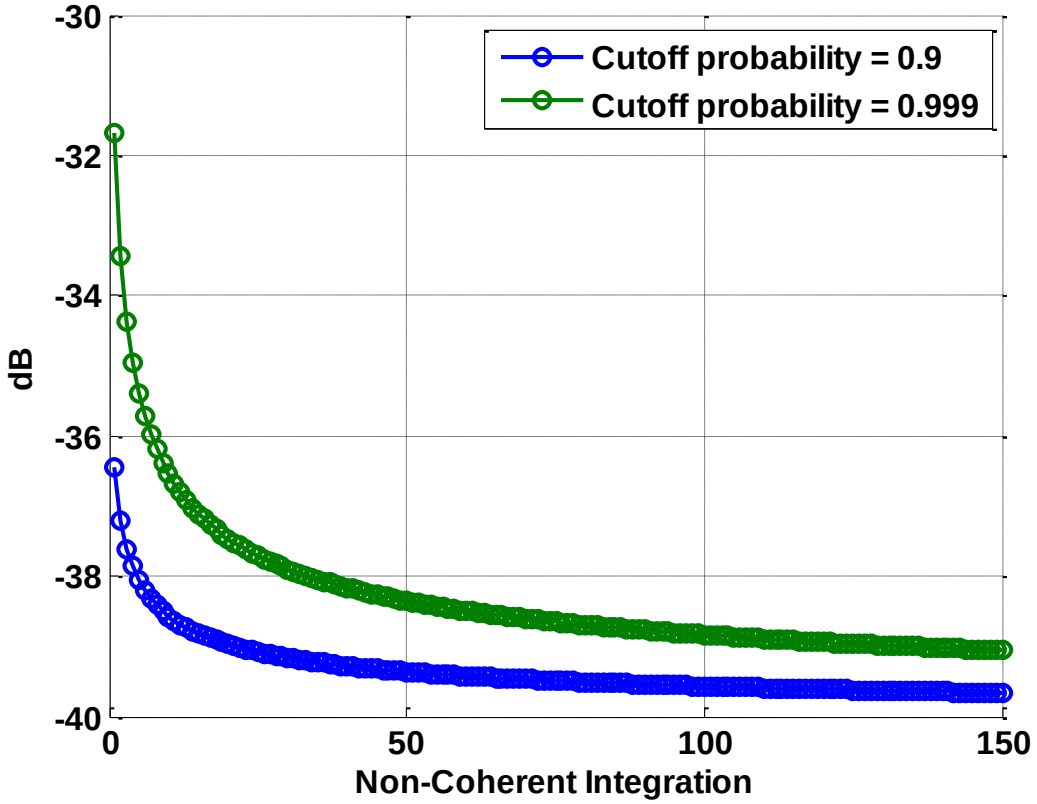

C/A Sidelobe

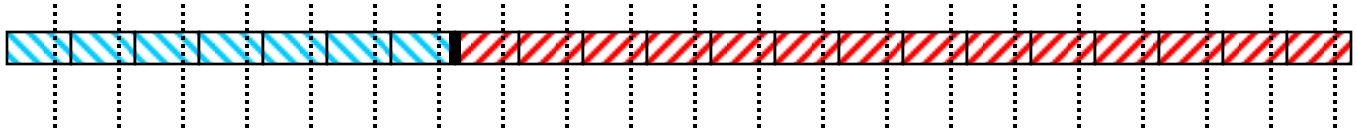

- **Because of the 20 repetitions per data bit, integration for N ms would results in about *N* – *P* summands being identical**
  - Where *P* = floor(*N*/ 20)
- **The remaining *P* summands will be equal or different based on a possible data transition**
- **In practice, get a mixture of *P* + 1 distributions (w = 0, . . . , *P*)**

$$\left(wY_1 + (N - P + w)Y_2 \right) / (2\,L\,N)$$

  - Each variable is a Chi-square with 2 degrees of freedom
- **For large *N*, we expect the distribution to become flat (independent of *N*)**
  - This quantifies how non-coherent integration helps against noise, but not a strong intra-system interferer

C/A Sidelobe Distribution

- **The tail cutoffs become flat**

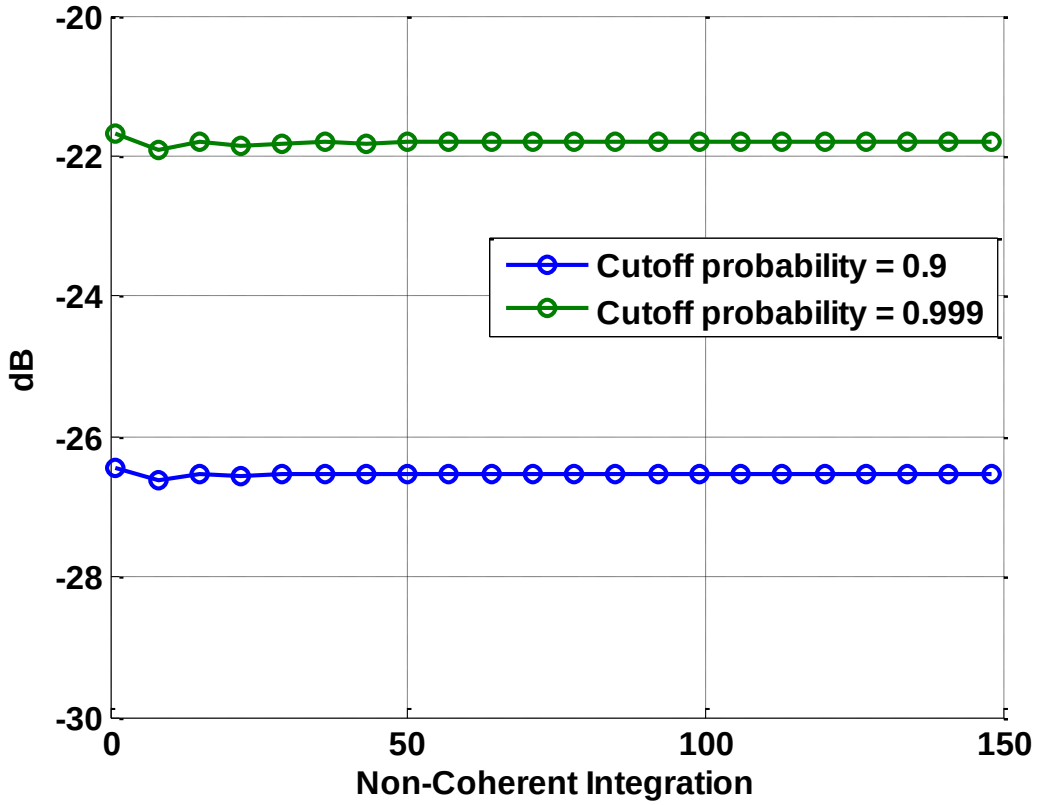

L5 Sidelobe

- **The types of variables depend on the bit transitions in the interfering pilot and data components**
- **We get 8 flavors of variables, each is a Chi-square with 4 degrees of freedom (assuming desired pilot and data sums)**
  - Because each interferer effects the desired pilot and data components the same
- **The distribution is a mixture based on the patterns of flavors distributed over the *N* summands**
  - Note that the flavors are not independent in time
- **This leads to a combinatorial explosion**
  - We use approximation methods to get close to the model distribution
  - We ignore the structure in the NH codes

A Pattern Example

- **Suppose this is the set of overlay signs for the interfering pilot and data components (*N* = 24 summands total)**
  - Eight possible flavors, up to sign (labeled 0, 1, . . ., 7)

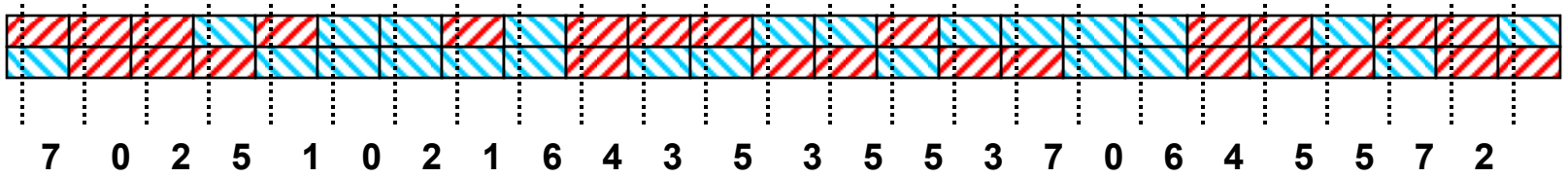

- **Grouping these patterns by type yields the normalized distribution**

$$\left(3Y_0 + 2Y_1 + 3Y_2 + 3Y_3 + 2Y_4 + 6Y_5 + 2Y_6 + 3Y_7\right) / (2 \cdot L \cdot 24)$$

  - Each Y_k is modeled as an independent Chi-square with 2 degrees of freedom
- **Next, "just" do this for all possible patterns**

L5 Sidelobe Results

- Region 1 is exhaustive over all possible patterns
- Region 2 is a mixture over likely patterns
- Region 3 is χ^2_{32} / (2 * 8 *L*) (assumes each flavor equally likely)
- Tails eventually also become flat

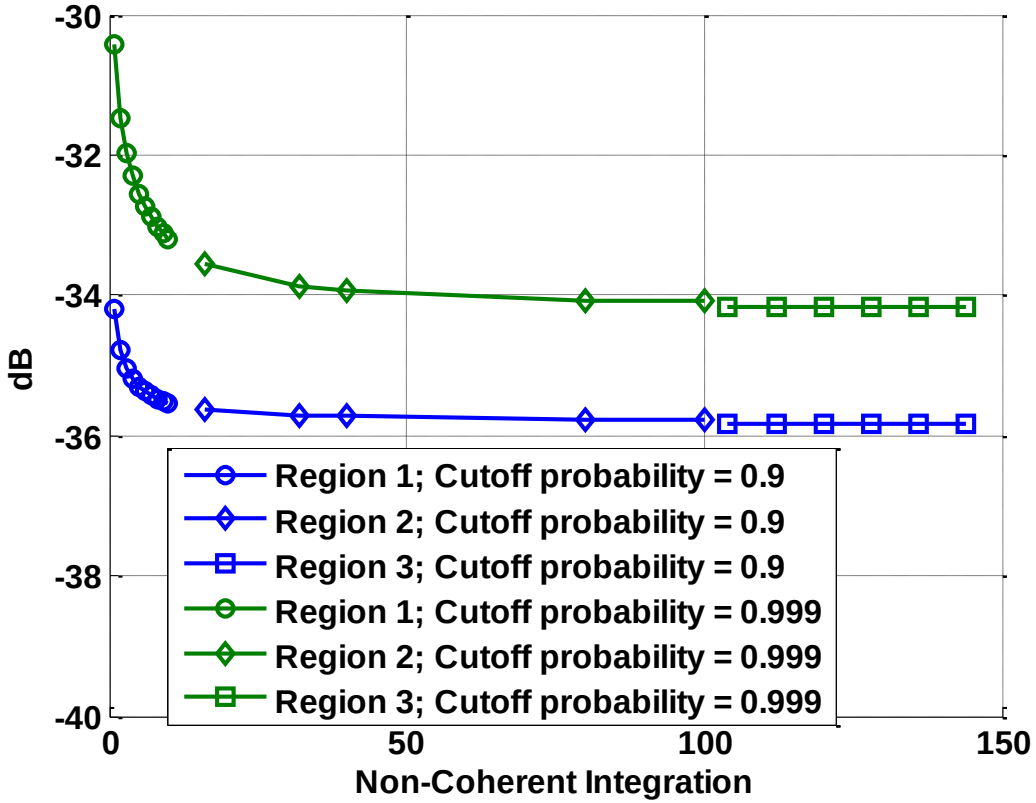

Outline

- Model basics
- Correlation coefficient
- Analysis via Gaussian quadratic forms
- The single interferer case
- **Conclusions**

Going Further

- **The modeling techniques can be readily applied to other GNSS systems**
  - L1C, L2C, etc.
- **Further work is needed to quantify the accuracy of the model**
  - For example, how much independence matters
- **Even so, its simplicity should be of value as a first order approximation**